

CrossMark
click for updates

Cite this: DOI: 10.1039/c5cy00577a

Received 20th April 2015,
Accepted 29th July 2015

DOI: 10.1039/c5cy00577a

www.rsc.org/catalysis

Mechanistic insights into the oxidative dehydrogenation of amines to nitriles in continuous flow

Emily C. Corker,^a Javier Ruiz-Martínez,^b Anders Riisager^a and Rasmus Fehrmann^{*a}

The oxidative dehydrogenation of various aliphatic amines to their corresponding nitrile compounds using RuO₂/Al₂O₃ catalysts in air was successfully applied to a continuous flow reaction. Conversions of amines (up to >99%) and yields of nitriles (up to 77%) varied depending on reaction conditions and the amine utilised. The presence of water was found to be important for the activity and stability of the RuO₂/Al₂O₃ catalyst. The Hammett relationship and *in situ* infrared spectroscopy were applied to divulge details about the catalytic mechanism of the oxidative dehydrogenation of amines over RuO₂/Al₂O₃ catalysts.

1. Introduction

Nitrile compounds boast many applications in organic synthesis and pharmaceutical chemistry.^{1–3} We have previously reported the oxidative dehydrogenation of ethylamine in continuous flow using RuO₂/Al₂O₃ catalysts, air as the oxidant and water as the reaction solvent for alternative, green synthesis of acetonitrile.⁴ However, the selective oxidative dehydrogenation of larger amines to nitriles in the presence of other functional groups may be of particular interest for the synthesis of larger chemical intermediates, where molecules may require a single functional group transformation in the presence of many other functional groups.

Previous methods for the synthesis of larger, more complex nitrile compounds have relied on stoichiometric reagents and batch chemistry.^{2,5–13} However, oxidation of alcohols in continuous flow using RuO₂/Al₂O₃ catalysts has been previously reported.¹⁴ In recent years there has been an emergence of flow chemistry for functional group transformations, both within laboratories and industry.^{15–17} The use of continuous flow processes offers advantages such as improved safety, efficient catalyst separation, improved space economy, reproducibility, automation and process reliability. Furthermore, our previous work has highlighted that the use of a continuous flow reaction for the oxidative dehydrogenation of amines allows the use of water as the reactant solution solvent, without enabling hydration of the product nitrile to its corresponding amide, thus improving the green credentials of the process. For this reason, the work on the

conversion of amines to nitriles presented here was performed in a gas-phase, continuous flow reaction setup.

In this work, we extend the applicability of our previous work concerning the oxidative dehydrogenation of simple amines in continuous flow using RuO₂/Al₂O₃ catalysts to include various aliphatic amines. In an effort to design a process that was as green as possible, water was our reactant solution solvent of choice, due to the limited solubility of some amine compounds in water, we also investigate the effect of changing the reactant solution solvent on the activity and stability of RuO₂/Al₂O₃ catalysts during oxidative dehydrogenation of amines in continuous flow.

Mizuno *et al.* have previously suggested a mechanism for the oxidative dehydrogenation of amines over RuO₂/Al₂O₃ catalysts in a batch process (Fig. 1).¹³ They conducted Hammett investigations and concluded that the reaction mechanism

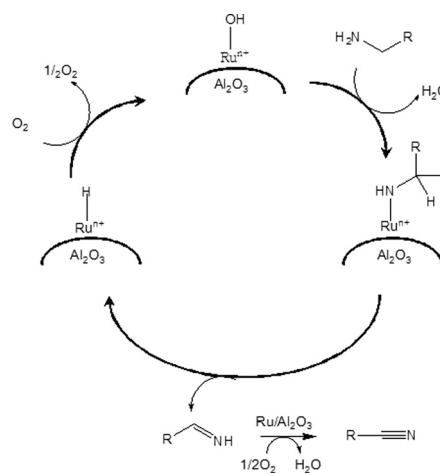


Fig. 1 Mechanism for the oxidative dehydrogenation of amines by RuO₂/Al₂O₃ catalysts, proposed by Mizuno *et al.*¹³

^a Centre for Catalysis and Sustainable Chemistry, Department of Chemistry, Technical University of Denmark, DK-2800, Kgs. Lyngby, Denmark.

E-mail: rf@kemi.dtu.dk; Fax: +45 4588 3136; Tel: +45 45252389

^b Group of Inorganic Chemistry and Catalysis, Department of Chemistry, Utrecht University, Universiteitsweg 99, 3584 CG Utrecht, The Netherlands

included formation of a carbocation-type intermediate species during oxidation and β -hydride elimination was the rate-determining step. Here, using the oxidative dehydrogenation of benzyl amines with various substituent groups, we present mechanistic investigations using the novel application of the Hammett relationship to results from continuous flow.

Previous investigations of the oxidative dehydrogenation of amines using heterogeneous catalysts have been limited to applications of catalysts to various reactants and kinetic studies of batch reactions.^{5,13,18} We combine the results from the Hammett relationship study in continuous flow with (to the best of our knowledge) the first *in situ* investigations of the oxidative dehydrogenation of amines over heterogeneous catalysts. We use results from Hammett investigations and *in situ* infrared (IR) spectroscopy to suggest an updated catalytic mechanism for the oxidative dehydrogenation of amines over $\text{RuO}_2/\text{Al}_2\text{O}_3$ catalysts.

2. Experimental detail

All chemicals for catalyst synthesis and testing were obtained from Sigma-Aldrich unless otherwise stated and used as received.

2.1 Catalyst synthesis

The $\text{RuO}_2/\text{Al}_2\text{O}_3$ catalyst was synthesised in a similar manner to previously reported,⁴ with a target Ru loading of 4.5 wt%. 2.78 g RuCl_3 hydrate (38–42 wt% Ru) was dissolved in 1.00 L of distilled water. 31.40 g Al_2O_3 (Saint-Gobain, BET surface area $256 \text{ m}^2 \text{ g}^{-1}$) was added to the solution to form a slurry which was stirred for 15 min. 1 M NaOH solution was added to the slurry to adjust the pH to 13.5. The slurry was then stirred at room temperature for 18 h. The resulting powder was filtered, washed with distilled water, dried at 140°C and calcined at 350°C in air for 3 h.

The $\text{RuO}_2/\text{Al}_2\text{O}_3$ catalyst used for *in situ* IR spectroscopy was prepared in a similar way to the catalyst used for catalytic testing, described above. However, in order to decrease light absorbance by the catalyst, increase transmission to the detector and slow the reaction to aid detection of short lived intermediates, a catalyst with a low Ru loading (0.7 wt%) was synthesised and used for the *in situ* IR experiments. 0.037 g RuCl_3 hydrate was dissolved in 86 ml of distilled water. 2.93 g Al_2O_3 (Saint Gobain, BET surface area $256 \text{ m}^2 \text{ g}^{-1}$) was added to the solution to form a slurry which was stirred for 15 min. 1 M NaOH solution was added to the slurry to adjust the pH to 13.5. The slurry was then stirred at room temperature for 18 h. The resulting powder was filtered, washed with distilled water and dried at 140°C .

2.2 Catalytic testing

Oxidative dehydrogenation of various benzyl and linear aliphatic amines to their corresponding nitriles (Fig. 2) were conducted under continuous flow conditions in a fixed bed, stainless steel reactor (a schematic diagram of the

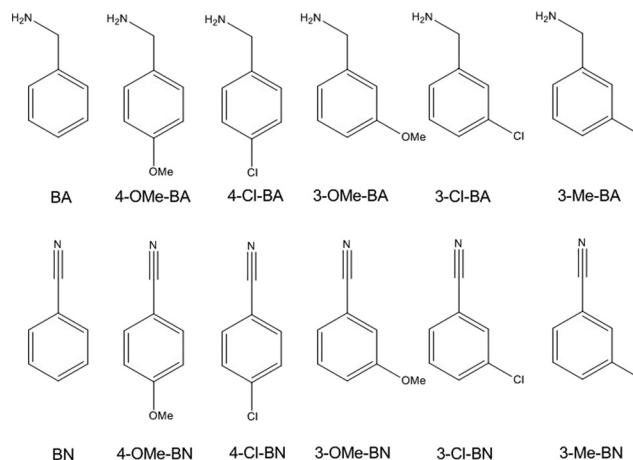


Fig. 2 Benzyl amines utilized in this work (top) and their corresponding nitriles (bottom).

continuous flow set up used can be seen in Fig. 3) charged with 0.300 g catalyst (180–350 μm size fraction).

During the reaction, the reactant liquid containing 10 wt% desired amine, 2 wt% dioxane (internal standard) in water, acetonitrile (AcCN) or a 50 : 50 mix of water : AcCN was introduced by an HPLC pump (Mikrolab) to the reactor (WHSV = 1.0 h^{-1} , GHSV = 1200 h^{-1}) where it was evaporated at the inlet. Air and He (AGA, grade 5.0) were introduced by mass flow controllers (Brooks Smart Mass Flow) and the total gas flow (including reactant, internal standard and solvent vapour) was kept constant at 150 ml min^{-1} in all experiments. All experiments were performed at a total pressure of 1 bar and the reaction temperatures used were 250 and 225°C . The reaction temperature was measured using a thermocouple outside the reactor at equal height to the catalyst bed. The product mixture was condensed in ice-cold ethanol, collected every hour and analysed by an offline GCMS (Agilent 6890, Column CP-Chirasil-Dex CB) equipped with an FID and mass spectrometer. Product ratios were determined in reference to the internal standard and a calibration curve produced using the reactant material.

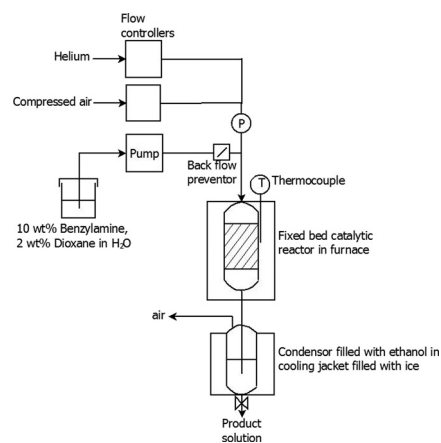


Fig. 3 Schematic diagram of the continuous flow set up used for the oxidative hydrogenation of amines to nitriles.

2.3 *In situ* IR spectroscopy

5 mg of RuO₂/Al₂O₃ (0.7 wt% Ru) was pressed into a thin pellet and loaded into an *in situ* cell (Linkam FTIR 600) equipped with a temperature controller (Linkam TMS 93). The *in situ* cell was placed into a Tensor 37 IR spectrometer equipped with a liquid N₂ cooled detector.

The RuO₂/Al₂O₃ catalyst pellet in the *in situ* cell was placed in a flow of 20 ml min⁻¹ O₂ and heated to 350 °C at a rate of 15 °C min⁻¹. The pellet was kept at this temperature for 150 min before cooling to the reaction temperature, 225 °C, at a rate of 15 °C min⁻¹. Throughout the pretreatment step, IR spectra were recorded every minute. Once the pretreatment was complete, the reaction gas was diverted through a bubbler containing a solution of 70 wt% ethylamine in water cooled to -20 °C using an ice/salt bath. The catalyst was exposed to ethylamine for 1 h before the gas flow was diverted back to oxygen only. Throughout the exposure to ethylamine and post-reaction purging, infrared spectra were recorded every minute.

3. Results and discussion

3.1 Catalytic testing

3.1.1 Application of oxidative dehydrogenation to a variety of amines and effects of reactant solution solvent change. All the tested amines were successfully converted to their corresponding nitrile using continuous flow oxidative dehydrogenation in air over RuO₂/Al₂O₃ catalysts, as shown by the results presented in Table 1. In general (Table 1, entries 1–7), high conversions were achieved (94–100%) and nitrile yields of 20–70%. For the oxidative dehydrogenation of each amine, analogous by-products were obtained with small amounts of aldehyde and larger amounts of *N*-substituted imines (see Fig. 4). No products of additional side reactions were observed, suggesting that the process was tolerant to the presence of the functional groups tested.

Activities for the oxidative dehydrogenation of each amine are reported in Table 1 and were higher than those reported by Mizuno *et al.*¹³ For example, Mizuno *et al.* reported a rate of benzonitrile production of 0.0040 mol g⁻¹ h⁻¹, 38% lower than the rate of benzonitrile production

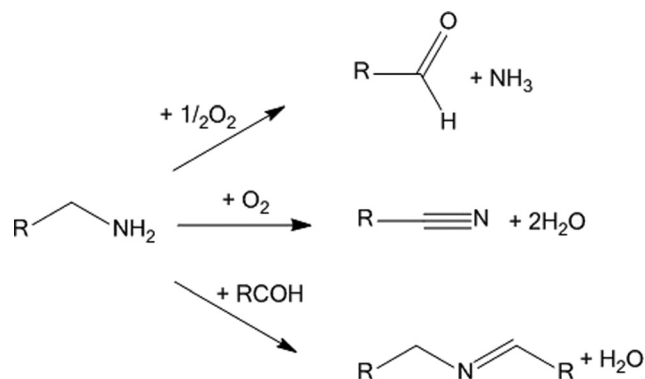


Fig. 4 Formation of products and by-products during the oxidative dehydrogenation of amines over RuO₂/Al₂O₃ catalysts in continuous flow.

reported in Table 1. However, for some reactions, the amine conversions, nitrile production rates and yields decreased significantly during the 5 h on stream, indicating low catalyst stability. Low catalyst stability may be caused by degradation by ammonia (formed during by-product formation) or fouling. Catalyst deactivation in continuous flow was also observed by Root *et al.* during the oxidation of alcohols using RuO₂/Al₂O₃ catalysts. Root *et al.* concluded that the catalyst was deactivated due to binding of carboxylic acids to the catalyst.¹⁴

A number of reaction conditions were tested and the results presented in Table 1 represent the optimal recorded conditions for the oxidative dehydrogenation of each amine. For the oxidative dehydrogenation of benzylamine, nitrile yields and catalyst stability were all found to be significantly improved when water was used as the reactant solution solvent, rather than AcCN (Fig. 5). When a 50:50 H₂O:AcCN (w/w) mix was used as the reactant solution solvent, nitrile yields and catalyst stability were between the ones obtained for the pure reactant solution solvents. A similar effect was observed for all the tested amines; when water was added to the reactant solution solvent then conversions, nitrile yields and catalyst stability were significantly improved for the oxidative dehydrogenation of both aliphatic and benzyl amines (Fig. 5 and 6).

Table 1 Results of catalytic testing for the oxidative dehydrogenation of various amines in continuous flow^a

Entry	Reactant	Product	Temperature (°C)	Reactant solution solvent	O ₂ : amine	Activity ^b (mol g ⁻¹ h ⁻¹)	Conversion ^b (%)	Yield ^b (%)	Conversion ^c (%)	Yield ^c (%)
1	BA	BN	250	H ₂ O	14	0.0065	>99	75	>99	70
2	3-Me-BA	3-Me-BN	250	H ₂ O/AcCN	14	0.0048	>99	75	86	34
3	4-MeO-BA	4-MeO-BN	250	H ₂ O/AcCN	14	0.0057	>99	77	>99	20
4	3-MeO-BA	3-MeO-BN	250	H ₂ O/AcCN	14	0.0042	98	57	62	21
5	3-Cl-BA	3-Cl-BN	250	H ₂ O/AcCN	14	0.0045	>99	61	77	25
6	4-Cl-BA	4-Cl-BN	250	AcCN	14	0.0023	94	41	75	29
7 ^d	Ethylamine	AcCN	225	H ₂ O	3	0.0169	>99	76	>99	75
8	Butylamine	Butanenitrile	225	H ₂ O	10	0.0048	41	34	21	18
9	Pentylamine	Pentanenitrile	225	H ₂ O	12	0.0014	68	54	46	29

^a Reaction conditions: WHSV_{amine} = 1 h⁻¹, total gas flow = 150 ml min⁻¹, 0.300 g RuO₂/Al₂O₃ (350 °C calcined), 1 bar. ^b After 1 h of reaction. ^c After 5 h of reaction. ^d Ethylamine results from previously published work.⁴

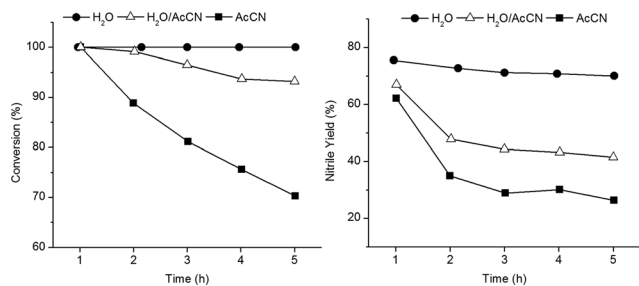


Fig. 5 Conversion and nitrile yield with increasing reaction time for the oxidative dehydrogenation of benzylamine in H₂O, AcCN and 50:50 (w/w) H₂O:AcCN. Reaction conditions: temperature = 250 °C, O₂:benzylamine = 14.4, WHSV_{benzylamine} = 1 h⁻¹, total gas flow = 150 ml min⁻¹, 0.300 g RuO₂/Al₂O₃ (350 °C calcined), 1 bar.

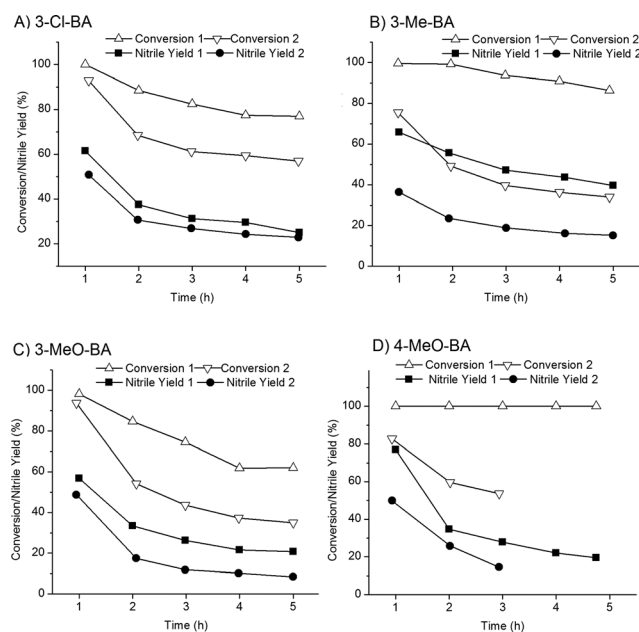


Fig. 6 Conversion and nitrile yield with increasing reaction time for the oxidative dehydrogenation of benzyl amines (A) 3-Cl-BA, B) 3-Me-BA, C) 3-MeO-BA, D) 4-MeO-BA in 50:50 (w/w) H₂O:AcCN (1) or AcCN only (2). Reaction conditions: temperature = 250 °C (except for the oxidative dehydrogenation of 4-MeO-BA in AcCN which was conducted at 225 °C, due to persistent reactor blocking at 250 °C) O₂:amine = 14.4, WHSV_{amine} = 1 h⁻¹, total gas flow = 150 ml min⁻¹, 0.300 g RuO₂/Al₂O₃ (350 °C calcined), 1 bar.

The oxidative dehydrogenation of butylamine and pentylamine resulted in considerably lower amine conversions than expected (Table 1, entries 8 and 9). In similarity to the oxidative dehydrogenation of the benzyl amines, conversions were improved significantly by increased O₂:amine and by use of H₂O as the reactant solution solvent (Fig. 7). However, conversions remained significantly lower than those observed for the oxidative dehydrogenation of benzyl amines and those previously observed for oxidative dehydrogenation of ethylamine.⁴

3.1.2 Hammett studies. To avoid comparisons of rates of reaction at 100% conversion, the reaction temperature was reduced to 225 °C and amine conversions decreased

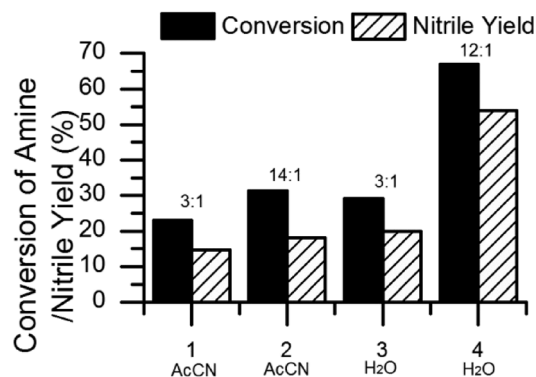


Fig. 7 Initial conversion of pentylamine (after 1 h) and initial yields of pentane nitrile under various reaction conditions. 1) AcCN solvent, O₂:pentylamine = 3:1, 2) AcCN solvent, O₂:pentylamine = 14:1, 3) H₂O solvent, O₂:pentylamine = 3:1, 4) H₂O solvent, O₂:pentylamine = 12:1. Reaction conditions: temperature = 225 °C, WHSV_{pentylamine} = 1 h⁻¹, total gas flow = 150 ml min⁻¹, 0.300 g RuO₂/Al₂O₃ (350 °C calcined), 1 bar.

accordingly (49–82%). Rates of conversion were determined and a Hammett plot was produced (Fig. 8).

The oxidative dehydrogenation of benzyl amines with positive sigma values resulted in lower initial rates of reaction than for oxidative dehydrogenation of unsubstituted benzylamine, as expected based on the results of Mizuno *et al.*¹³ However, it would also be expected that the oxidative dehydrogenation of amines with a negative sigma value would result in higher rates of reaction than observed for benzylamine, but this was not the case. The low observed rates for the oxidative dehydrogenation of benzyl amines with negative sigma values may be due to steric hindrance caused by the presence of larger side groups or a change in mechanism caused by electron-rich substituents.

After several repeated experiments, the results of the oxidative dehydrogenation of 4-MeO-BA and 3-Me-BA were considered outliers and the ρ value was determined to be -1.04

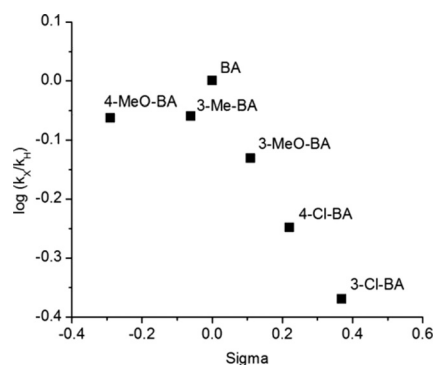


Fig. 8 Sigma value of various amines against $\log(k_X/k_{BA})$, where k_X = initial rate of conversion of amine with substituent group X (mol g⁻¹ h⁻¹) during oxidative dehydrogenation. Reaction conditions: temperature = 225 °C, O₂:amine = 14.4, WHSV_{amine} = 1 h⁻¹, total gas flow = 150 ml min⁻¹, 0.300 g RuO₂/Al₂O₃ (350 °C calcined), AcCN solvent, 1 bar.

($R^2 = 0.99$) from linear regression of the remaining points. A negative ρ value is indicative of electron flow away from the aromatic ring in the rate determining step of the reaction.

Mizuno *et al.* applied the Hammett relationship to the oxidative dehydrogenation of amines using Brown–Okamoto σ constants,^{13,19} however we found a better relationship with the traditional Hammett relationship. The better fit of the results with the traditional Hammett σ constants compared to the Brown–Okamoto σ constants suggests that positive charge is not formed during the rate determining step. Mizuno *et al.* found a much smaller ρ value (-0.154), indicating that under the conditions applied in our continuous flow process, the substituents have a greater electronic effect than in the batch process utilized by Mizuno *et al.* The differences between ρ values and appropriate σ constants may be due to a difference in rate determining steps of the batch and continuous flow processes, or a result of variation in reaction conditions including temperature, pressure and solvents present.

We propose that the rate determining step of the oxidative dehydrogenation of amines in continuous flow involves the removal of a hydrogen atom from the carbon atom adjacent to the amine group, either by β -hydride elimination, in agreement with Mizuno *et al.*, or by another mechanism.

3.2 *In situ* IR spectroscopy

The IR spectrum of the fresh $\text{RuO}_2/\text{Al}_2\text{O}_3$ catalyst (Fig. 9) is dominated by the presence of water and surface hydroxyls, as shown by the presence of a broad band in the OH stretching region ($3700\text{--}3000\text{ cm}^{-1}$), which can be assigned to surface hydroxyl groups and water.^{20–23} The presence of physisorbed water is confirmed by the presence of a band that may be assigned to an HOH bend at 1645 cm^{-1} .^{21,22} Also present in the spectrum of the fresh catalyst $\text{RuO}_2/\text{Al}_2\text{O}_3$ are bands at 1401 and 1542 cm^{-1} , which are probably due to the presence of surface carbonate and carboxylate species formed due to the adsorption of atmospheric CO_2 on the catalyst surface.²⁴

Calcination of the $\text{RuO}_2/\text{Al}_2\text{O}_3$ catalyst significantly reduced the OH contributions to the spectra, though a broad OH stretching band remained at $3000\text{--}3750\text{ cm}^{-1}$, due to the

presence of persistent surface OH groups. The band at 1645 cm^{-1} (assigned to an HOH bend due to the presence of water) was no longer present after calcination, suggesting that all physisorbed water was removed during calcination. The observed IR spectra therefore agree with the postulation that calcination at $350\text{ }^\circ\text{C}$ in O_2 leads to a less hydrated $\text{RuO}_2/\text{Al}_2\text{O}_3$ catalyst. Contributions to the spectra from carbonate and carboxylate species were also reduced, with much smaller blue shifted bands present at 1853 , 1576 and 1460 cm^{-1} , as seen in Fig. 9.

Upon exposure of the $\text{RuO}_2/\text{Al}_2\text{O}_3$ catalyst to ethylamine rapid changes were observed in the IR spectra, as shown by Fig. 10. Within 1 min of exposure to ethylamine, IR absorption bands developed in the $2750\text{--}3100\text{ cm}^{-1}$ and $1200\text{--}1600\text{ cm}^{-1}$ regions. IR absorption bands in the $2750\text{--}3100\text{ cm}^{-1}$ region can be broadly assigned to C–H stretches,²⁰ which confirm the presence of ethylamine in the reaction cell. Specifically the peaks at 2968 , 2942 , 2885 and 2855 cm^{-1} can be assigned to the CH_3 symmetric stretch, CH_2 symmetric stretch, CH_3 asymmetric stretch and CH_2 asymmetric stretch, respectively, indicating the presence of an ethyl group.²⁵ IR absorption bands in the complex $1200\text{--}1600\text{ cm}^{-1}$ region include CH_2 and CH_3 bending vibrations, C–C stretches and NH_2 scissoring at 1550 cm^{-1} .^{20,26,27}

In comparison to the freshly calcined catalyst a reduction in the intensity of the absorption bands at 1460 and 1853 cm^{-1} was observed in the IR spectra after 1 min of exposure to ethylamine. This suggests that ethylamine replaced carbonate and carboxylate species that were present on the catalyst surface prior to exposure to ethylamine.

After the $\text{RuO}_2/\text{Al}_2\text{O}_3$ catalyst had been under reaction conditions for 5 min, there were no absorption bands present in the IR spectra indicative of the presence of an aldehyde or nitrile compound. However, an imine may have been present as a band was formed at 1588 cm^{-1} after 4.6 min under reaction conditions, which can be assigned to a characteristic imine C=N stretching band.²⁰ As no IR band that could be attributed to an aldehyde was detected, we suggest that the detected imine was an unsubstituted imine and intermediate for the synthesis of acetonitrile.

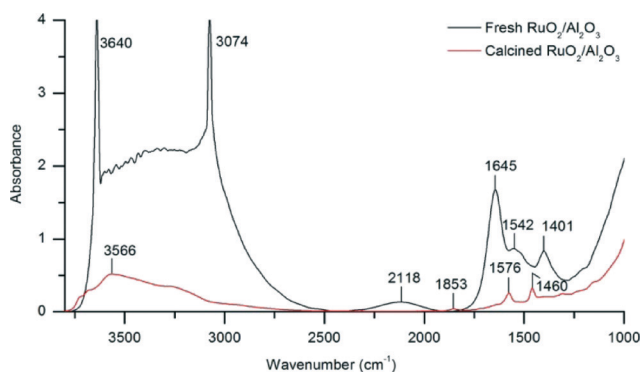


Fig. 9 IR spectra of fresh $\text{RuO}_2/\text{Al}_2\text{O}_3$ catalyst and catalyst calcined at $350\text{ }^\circ\text{C}$ for 150 min in $20\text{ ml min}^{-1}\text{ O}_2$.

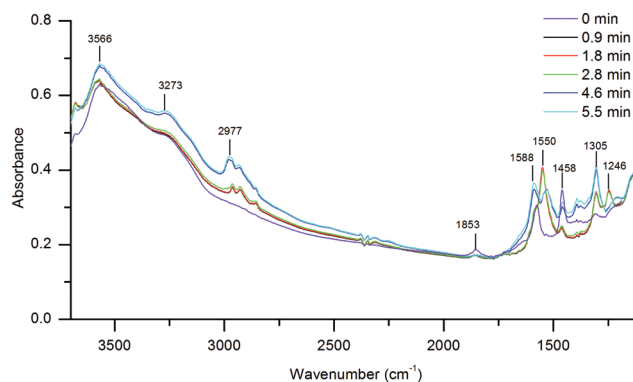


Fig. 10 IR spectra of $\text{RuO}_2/\text{Al}_2\text{O}_3$ catalyst during exposure to aqueous EtNH_2 solution (70 wt%) in $20\text{ ml min}^{-1}\text{ O}_2$ at $225\text{ }^\circ\text{C}$ after 0, 0.9, 1.8, 2.8, 4.6 and 5.5 min.

The IR spectra of the $\text{RuO}_2/\text{Al}_2\text{O}_3$ catalyst continued to change and develop for the entire 60 min under reaction conditions, as can be seen in Fig. 11. Bands representative of acetonitrile, including the $\text{C}\equiv\text{N}$ stretching band at 2251 cm^{-1} , began to appear in the IR spectra after approximately 10 min under reaction conditions. As the band at 2251 cm^{-1} was strong and not overlapping with any other bands, it was possible to track the development of the $\text{C}\equiv\text{N}$ stretching band at 2251 cm^{-1} in the IR spectra and therefore the presence of acetonitrile in the reaction cell with time (see Fig. 12).

A band at 1647 cm^{-1} developed within the first 20 min of the reaction and continued to increase in intensity throughout the time under reaction conditions. The band at 1647 cm^{-1} and its shoulder at approximately 1675 cm^{-1} could be assigned to the NH_2 scissoring and $\text{C}=\text{O}$ stretch of acetamide,²⁸ respectively, which may be formed *via* hydration of acetonitrile due to the slow flow rate through the *in situ* cell. The formation of acetamide coupled with the reduction of the intensity of the $\text{C}\equiv\text{N}$ stretching band at 2251 cm^{-1} after 20 min under reaction conditions (Fig. 12) supports the suggestion that acetonitrile is hydrated to acetamide. There was no evidence for the presence of acetic acid in the *in situ* cell, which would result in the presence of a strong band at approximately 1710 cm^{-1} , corresponding to its $\text{C}=\text{O}$ stretch.^{20,26}

There was not a lot of change observed in the region of the IR spectra above 2750 cm^{-1} during the 60 min under reaction conditions, although various NH stretching bands may be expected. The lack of observable change in this region may be due to the broad OH stretching band masking other contributions to the IR spectra.

Though the reactant cell was purged with O_2 for over 100 min post reaction, the catalyst did not return to the freshly calcined state, as shown by the IR spectra in Fig. 13. Although many of the bands contributing to the spectra do appear reduced with increased purging time, as seen in Fig. 14, a variety of absorption bands indicating the presence of organic species on the catalyst surface can still be seen in

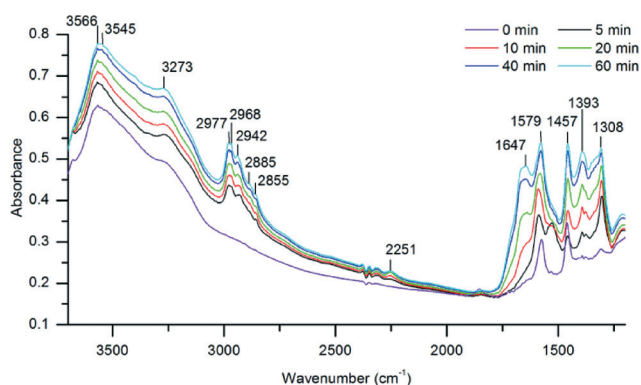


Fig. 11 IR spectra of $\text{RuO}_2/\text{Al}_2\text{O}_3$ catalyst during exposure to aqueous EtNH_2 solution (70 wt%) in $20\text{ ml min}^{-1}\text{ O}_2$ at $225\text{ }^\circ\text{C}$ after 0, 5, 10, 20, 40 and 60 min.

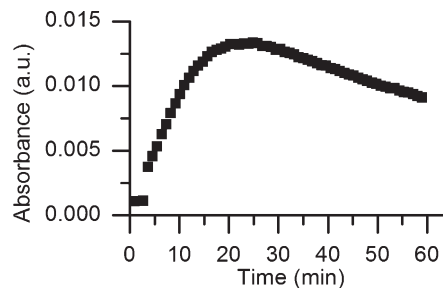


Fig. 12 $\text{C}\equiv\text{N}$ band absorbance (2251 cm^{-1}) development with time after exposure to aqueous EtNH_2 solution (70 wt%) in $20\text{ ml min}^{-1}\text{ O}_2$ at $225\text{ }^\circ\text{C}$.

the IR spectra of the catalyst after 60 min of purging, including CH stretches, $\text{C}\equiv\text{N}$ stretching band (2251 cm^{-1}) and many contributions in the fingerprint region of the spectra. The lack of significant reduction of the IR absorption bands in the spectra suggests that reactants and products are strongly bound to the surface of the catalyst. The large number of species strongly bound to the surface of the catalyst may explain the catalyst deactivation seen with increasing time on stream, in agreement with the conclusions of Root *et al.*¹⁴ Interestingly, the IR bands at 1579, 1647 and 1457 cm^{-1} appeared to increase with increased purging time, suggesting that residual acetonitrile and ethylamine were converted to other species including acetamide during the purging period.

3.3 Proposal of catalytic mechanism

Combining the results of our Hammett studies and *in situ* IR spectroscopy, we propose the catalytic mechanism presented in Fig. 15. In agreement with Mizuno *et al.*¹³ we suggest that the amine compound binds to the ruthenium centre *via* the amine group and that an imine intermediate seems likely.

Mizuno *et al.* suggest the presence of a ruthenium hydride species in the mechanism of oxidative dehydrogenation of amines over $\text{RuO}_2/\text{Al}_2\text{O}_3$ catalysts.¹³ However, the presence of a ruthenium hydride species in a highly oxidising

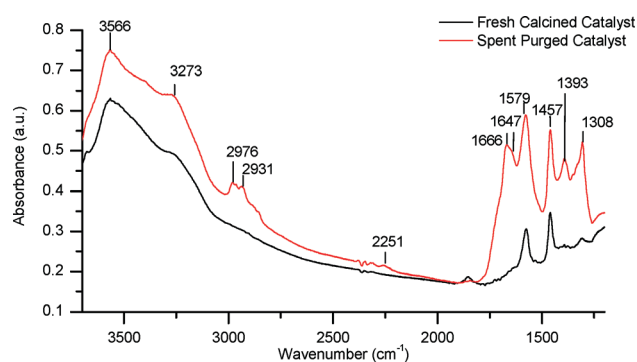


Fig. 13 IR spectra of $\text{RuO}_2/\text{Al}_2\text{O}_3$ catalyst after 100 min of post-reaction purging with $20\text{ ml min}^{-1}\text{ O}_2$ at $225\text{ }^\circ\text{C}$ and comparison to the freshly calcined catalyst.

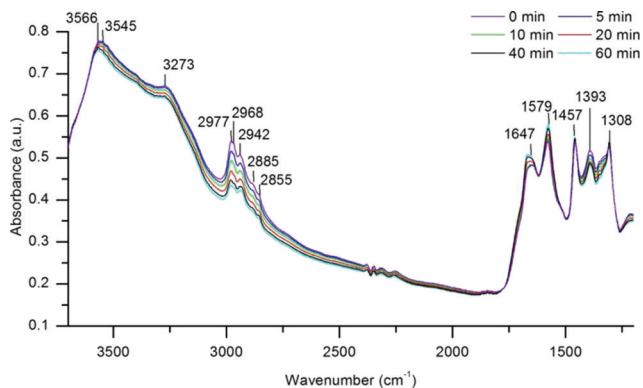


Fig. 14 IR spectra of $\text{RuO}_2/\text{Al}_2\text{O}_3$ catalyst during post-reaction purging with $20 \text{ ml min}^{-1} \text{ O}_2$ at $225 \text{ }^\circ\text{C}$.

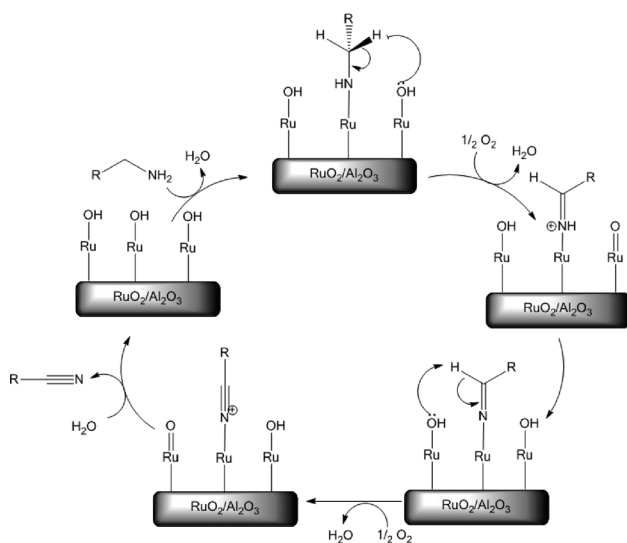


Fig. 15 Schematic diagram of the proposed mechanism for oxidative dehydrogenation of amines over $\text{RuO}_2/\text{Al}_2\text{O}_3$. Ruthenium atoms represented here are assumed to be surface atoms of the RuO_2 lattice.

environment seems unlikely. If a ruthenium hydride species is present for sufficient time to be detected by IR spectroscopy, we would expect to see a Ru–H stretching band in the IR spectra at approximately $1800\text{--}2000 \text{ cm}^{-1}$.^{29,30} Although a peak was present at 1853 cm^{-1} in the IR spectrum of the fresh catalyst, the peak was gone after 5 min under reaction conditions and no new peaks were formed in the $1800\text{--}2000 \text{ cm}^{-1}$ region during the entire time under reaction conditions. Therefore, we cannot substantiate the claim that a ruthenium hydride intermediate exists. As an alternative, we suggest that the surface hydroxide groups of the active $\text{RuO}_2/\text{Al}_2\text{O}_3$ catalysts play an active role in the removal of hydrogen from the amine.

Our work has suggested that stable and active $\text{RuO}_2/\text{Al}_2\text{O}_3$ catalysts for the oxidative dehydrogenation of amines rely on the presence of water. In our proposed mechanism, we suggest that water is necessary to regenerate the catalyst active site after the reaction has occurred (Fig. 15).

4. Conclusions

In this work, a variety of aliphatic nitriles were synthesised by the oxidative dehydrogenation of their corresponding amines in air and using $\text{RuO}_2/\text{Al}_2\text{O}_3$ catalysts under continuous flow conditions. The oxidative dehydrogenation of the benzyl amines occurred with varying degrees of success, with conversions ranging between 18–100% and nitrile yields ranging between 6–76%, depending on the amine used as the reactant and the reaction conditions applied. By far the best reaction conditions for the oxidative dehydrogenation of benzyl amines employed a reaction temperature of $250 \text{ }^\circ\text{C}$ and a $\text{H}_2\text{O}/\text{AcCN}$ mixture or H_2O only reactant solution solvent, where possible. Under these conditions, all the benzyl amines were oxidatively dehydrogenated to the corresponding nitrile with initial conversions over 98% and initial nitrile yields of 48–78% depending on the amine used. The presence of water in the reaction was found to improve conversion, nitrile yields and stability of the reaction over the 5 h tested.

The oxidative dehydrogenation of linear aliphatic amines was less successful, with low conversions (6–70%) and low nitrile yields (4–54%). The maximum achieved conversions and yields were obtained using a reaction temperature of $225 \text{ }^\circ\text{C}$, high O_2 :amine ratio (10–12:1) and H_2O as the reactant solution solvent.

The IR spectra observed during the oxidative dehydrogenation of ethylamine and interpreted in this work allowed observation of the order in which products and by-products of the oxidative dehydrogenation of ethylamine were produced. The results support the suggestion that ethylamine dehydrogenation to acetonitrile occurs *via* an imine compound. Furthermore, the later development of the spectra to include IR absorption bands that can be assigned to acetamide, supports the suggestion that acetamide by-product is formed by the hydration of acetonitrile when the reaction is occurring under a low gas flow. The presence of a ruthenium hydride species could not be confirmed using IR spectroscopy and an alternative catalytic mechanism was proposed.

Acknowledgements

The authors gratefully acknowledge funding from the European Community's Seventh Framework Programme [FP7/2007–2013] for SYNFLOW under grant agreement no. NMP2-LA-2010-246461.

References

- 1 F. F. Fleming, L. Yao, P. C. Ravikumar, L. Funk and B. C. J. Shook, *Med. Chem.*, 2010, **53**, 7902–7917.
- 2 D. T. Mowry, *Chem. Rev.*, 1948, **42**, 189–283.
- 3 M. North, in *Comprehensive Organic Functional Group Transformations, Volume 3*, ed. G. Pattenden, Elsevier, Amsterdam, 1995, pp. 611–640.
- 4 E. C. Corker, U. V. Mentzel, J. Mielby, A. Riisager and R. Fehrmann, *Green Chem.*, 2013, **15**, 928–933.

- 5 R. V. Jagadeesh, H. Junge and M. Beller, *ChemSusChem*, 2015, **8**, 92–96.
- 6 W. Yin, C. Wang and Y. Huang, *Org. Lett.*, 2013, **15**, 1850–1853.
- 7 H. Shimojo, K. Moriyama and H. Togo, *Synthesis*, 2013, **45**, 2155–2164.
- 8 H. Veisi, *Synthesis*, 2010, 2631–2635.
- 9 F.-E. Chen, Y.-Y. Li, M. Xu and H.-Q. Jia, *Synthesis*, 2002, 1804–1806.
- 10 T. Oishi, K. Yamaguchi and N. Mizuno, *Top. Catal.*, 2010, **53**, 479–486.
- 11 T. Oishi, K. Yamaguchi and N. Mizuno, *Angew. Chem., Int. Ed.*, 2009, **48**, 6286–6288.
- 12 J. Augustine, A. Bombrun and R. Atta, *Synlett*, 2011, 2223–2227.
- 13 K. Yamaguchi and N. Mizuno, *Angew. Chem., Int. Ed.*, 2003, **42**, 1480–1483.
- 14 D. S. Mannel, S. S. Stahl and T. W. Root, *Org. Process Res. Dev.*, 2014, **18**, 1503–1508.
- 15 J. Wegner, S. Ceylan and A. Kirschning, *Chem. Commun.*, 2011, **47**, 4583–4592.
- 16 C. Wiles and P. Watts, *Eur. J. Org. Chem.*, 2008, 1655–1671.
- 17 M. P. Dudukovic, F. Larachi and P. L. Mills, *Chem. Eng. Sci.*, 1999, **54**, 1975–1995.
- 18 C. Hammond, M. T. Schümperli and I. Hermans, *Chemistry*, 2013, **19**, 13193–13198.
- 19 H. C. Brown and Y. Okamoto, *J. Am. Chem. Soc.*, 1958, **80**, 4979–4987.
- 20 L. M. Harwood and T. D. W. Claridge, *Introduction to Organic Spectroscopy*, Oxford University Press, Oxford, 2008.
- 21 L. M. Kustov, *Top. Catal.*, 1997, **4**, 131–144.
- 22 W. Hanke and K. Möller, *Zeolites*, 1984, **4**, 244–250.
- 23 G. Lefèvre, M. Duc, P. Lepeut, R. Caplain and M. Fédoroff, *Langmuir*, 2002, **18**, 7530–7537.
- 24 A. M. Turek, I. E. Wachs and E. DeCanio, *J. Phys. Chem.*, 1992, **96**, 5000–5007.
- 25 B. H. Stuart, *Infrared Spectroscopy Fundamentals and Applications*, John Wiley & Sons, Ltd., 2004.
- 26 NIST Mass Spec Data Center, S. E. Stein, in *NIST Chemistry WebBook, NIST Standard Reference Database Number 69*, ed. P. J. Linstrom and W. G. Mallard, National Institute of Standards and Technology, Gaithersburg, 2014.
- 27 D. Zeroka, J. O. Jensen and A. C. Samuels, *J. Mol. Struct.: THEOCHEM*, 1999, **465**, 119–139.
- 28 E. Ganeshsrinivas, D. N. Sathyanarayana, K. Machida and Y. Miwa, *J. Mol. Struct.: THEOCHEM*, 1996, **361**, 217–227.
- 29 H. D. Kaesz and R. B. Saillant, *Chem. Rev.*, 1972, **72**, 231–281.
- 30 X. Wang and L. Andrews, *J. Phys. Chem. A*, 2009, **113**, 551–563.